

Figure S1: Diversity surrounding the causative substitution at the *tga1* locus.

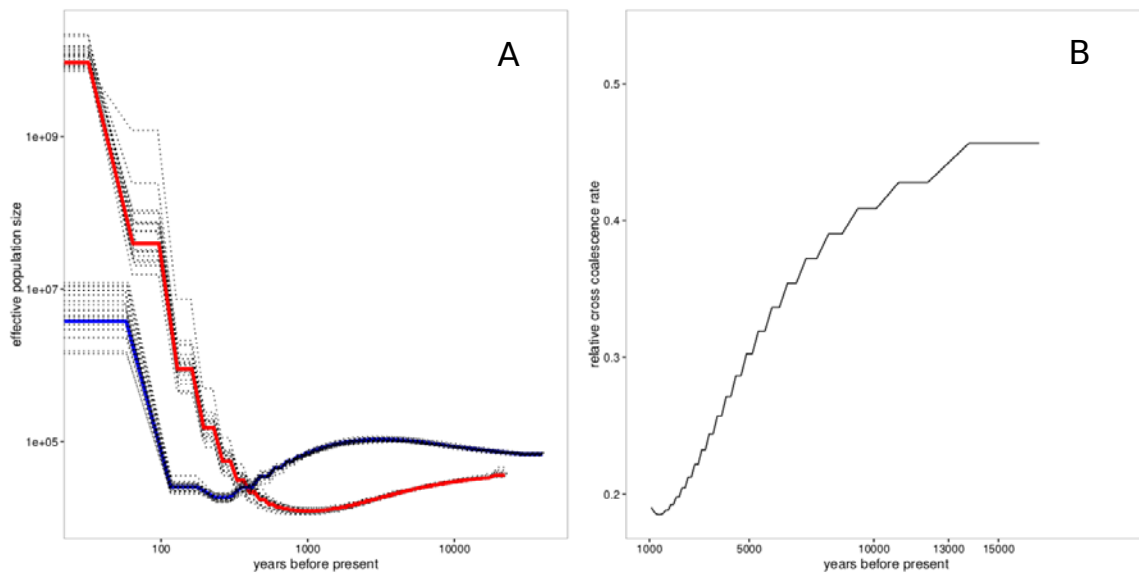


Figure S2: MSMC Analyses. Shown in **A** are effective population size estimates over time. Estimates are depicted as solid lines and bootstrap resampling is represented with dotted lines for both maize (red) and teosinte (blue). **B** depicts the relative cross-coalescence rate between maize and teosinte estimated using MSMC. In both panels, time is estimated assuming an annual generation time and a mutation rate of $\mu = 3 \times 10^{-8}$

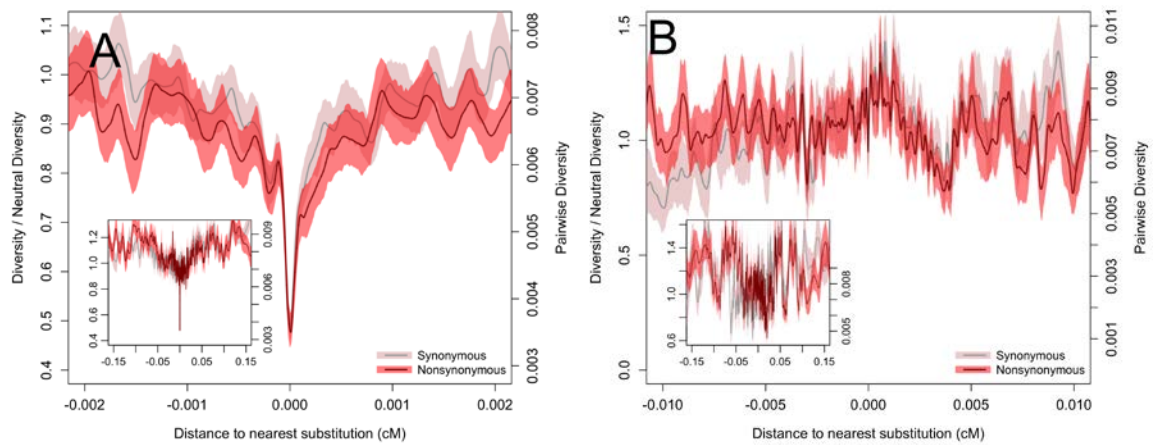


Figure S3: Pairwise diversity surrounding synonymous and nonsynonymous substitutions in maize at **A** highly conserved or **B** unconserved sites. Bootstrap-based 95% confidence intervals are depicted via shading. Inset plots depict a larger range on the x-axis.

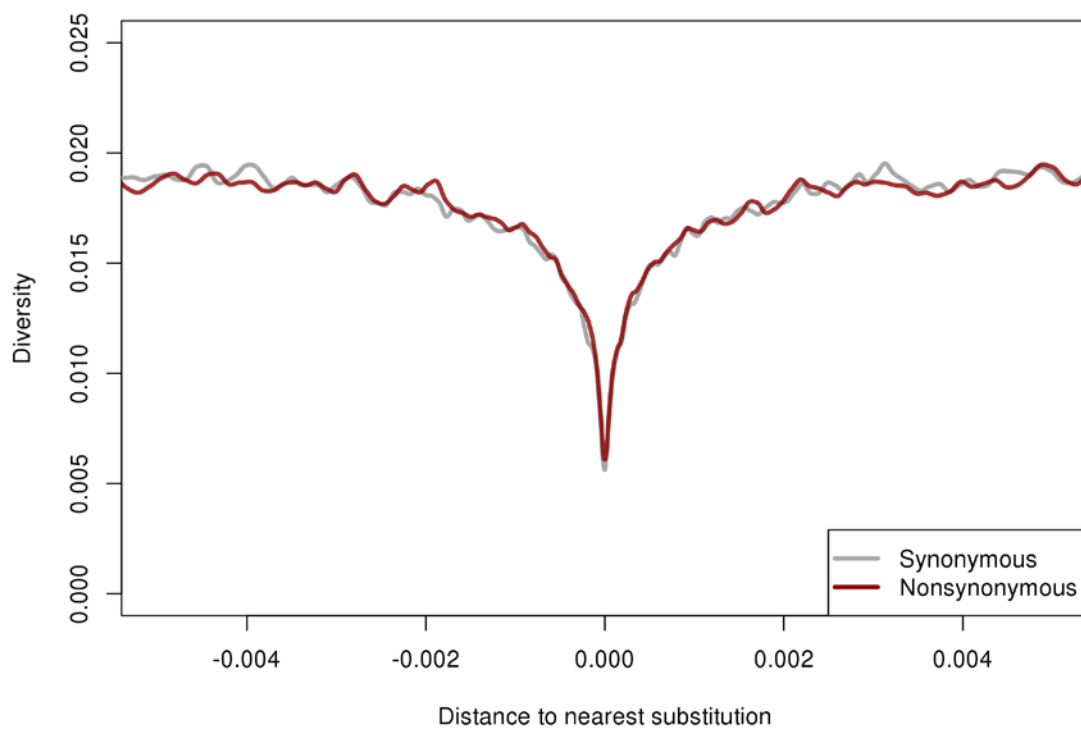


Figure S4: Singleton diversity surrounding synonymous and nonsynonymous substitutions in maize.

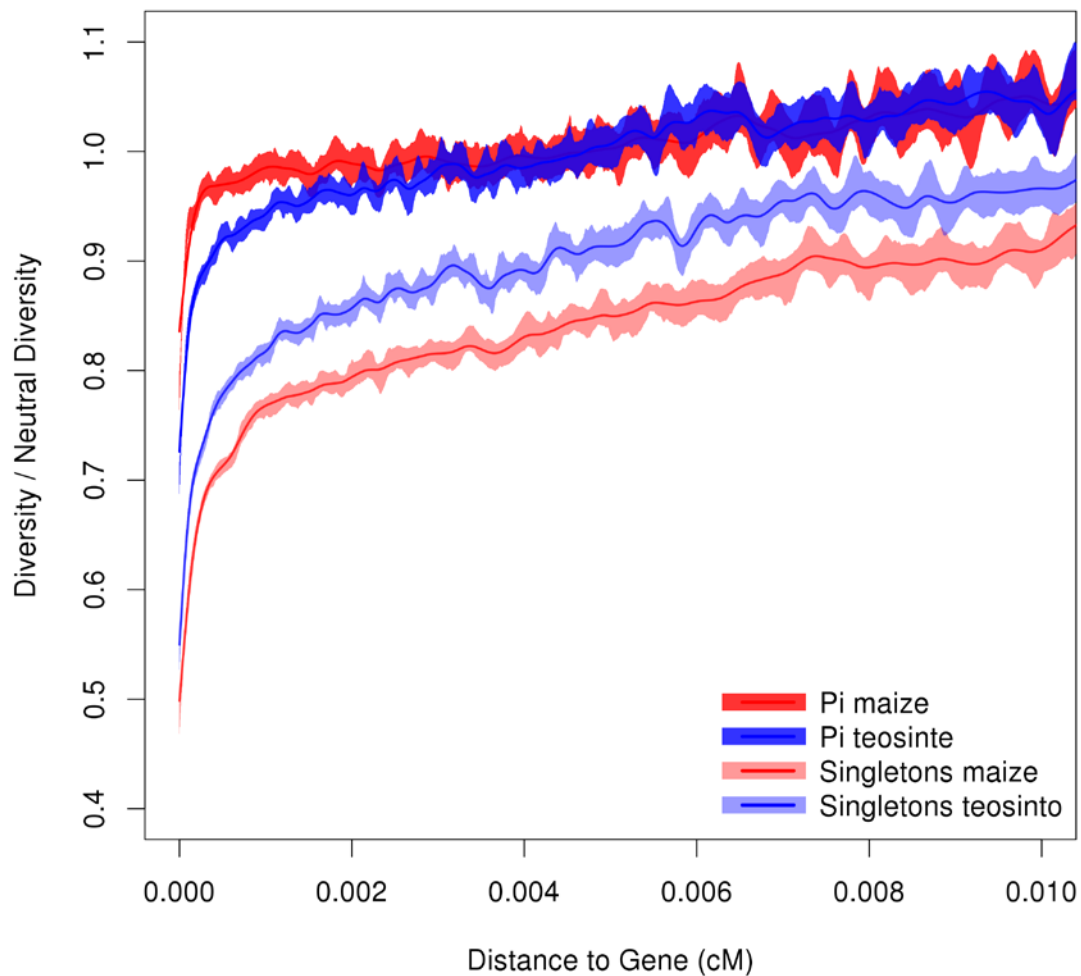


Figure S5: Relative diversity versus distance to nearest gene in maize and teosinte. Relative diversity is calculated by comparing to the mean diversity in all windows $\geq 0.02cM$ from the nearest gene. Lines depict cubic smoothing splines with smoothing parameters chosen via generalized cross validation and shading depicts bootstrap-based 95% confidence intervals.

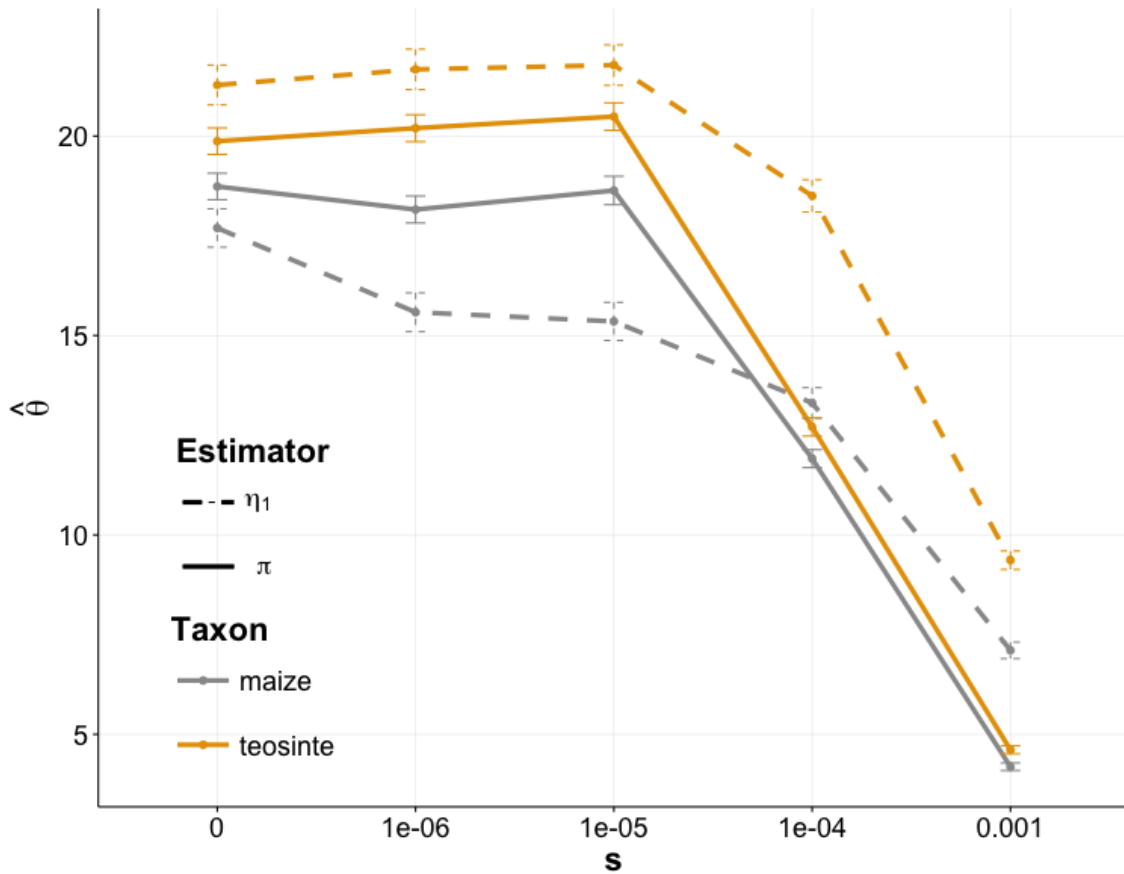


Figure S6: Simulations of diversity statistics in maize and teosinte with varying strengths of purifying selection. Points show the mean (\pm standard error) of the population mutation rate θ estimated by singletons (η_1) and pairwise differences (π).

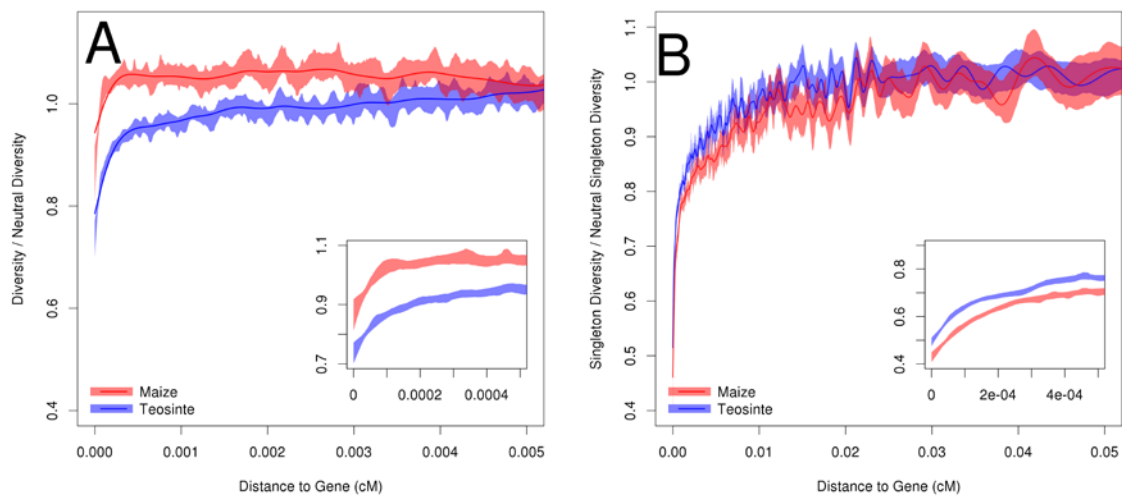


Figure S7: Relative level of diversity versus distance to the nearest gene, in maize and teosinte, based on only sites that do not show evidence of hard or soft sweeps according to H12. Two measures of diversity were investigated. **A** displays pairwise diversity, which is most influenced by intermediate frequency alleles and therefore depicts more ancient evolutionary patterns, and **B** depicts singleton diversity, influenced by rare alleles and thus depicting evolutionary patterns in the recent past. Bootstrap-based 95% confidence intervals are depicted via shading. Inset plots depict a smaller range on the x-axis.

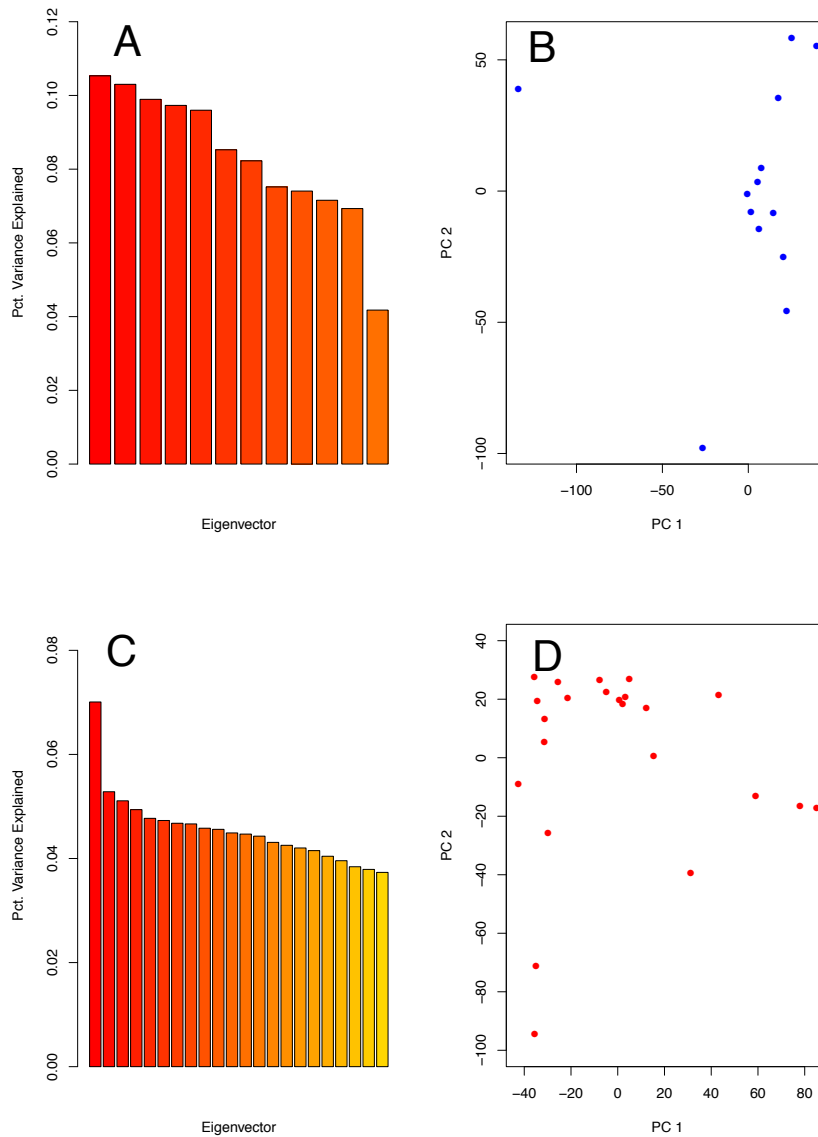


Figure S8: Principal component analysis of teosinte and maize individuals to ensure that no close relatives were inadvertently included in our study. Plots are based on a random sample of 10,000 SNPs. **A** displays the percentage of total variance explained by each principal component for teosinte, while **B** shows PC1 vs PC2 for all 13 teosinte individuals. Similarly, **C** depicts the percentage of total variance explained by each principal component for maize, and **D** shows PC1 vs PC2 for all 23 maize individuals.

Maize	Teosinte
BKN009	TIL01
BKN010	TIL02
BKN011	TIL03
BKN014	TIL04-TIP454
BKN015	TIL07
BKN016	TIL09
BKN017	TIL10
BKN018	TIL11
BKN019	TIL12
BKN020	TIL14-TIP498
BKN022	TIL15
BKN023	TIL16
BKN025	TIL17
BKN026	
BKN027	
BKN029	
BKN030	
BKN031	
BKN032	
BKN033	
BKN034	
BKN035	
BKN040	

Table S1: A list of maize and teosinte individuals included in this study. Sequencing and details were previously described by [22].

Parameter	Initial value	Upper bound	Lower bound
$\frac{N_b}{N_a}$	0.02	1×10^{-7}	2
$\frac{N_m}{N_a}$	3	1×10^{-7}	200
$\frac{T_b}{2N_a}$	0.04	0	1
$\frac{M_{mt}}{N_a}$	1×10^{-10}	1×10^{-7}	0.001
$\frac{M_{tm}}{N_a}$	1×10^{-10}	1×10^{-7}	0.001

Table S2: Parameters, initial values, and boundaries used for model-fitting with $\delta\alpha\delta i$. Parameters are shown in the units utilized by $\delta\alpha\delta i$, although in the text simplified units are reported.